Available online at www.sciencedirect.com
ScienceDirect
Geomorphology 100 (2008) 453–464
GEOMORPHOLOGY
www.elsevier.com/locate/geomorph

Landform classification from a digital elevation model and satellite imagery

Hossein Saadat [a], Robert Bonnell [a,*], Forood Sharifi [b], Guy Mehuys [a], Mohammad Namdar [b], Sasan Ale-Ebrahim [b]

[a] Department of Bioresource Engineering, McGill University, Macdonald Campus 21, 111 Lakeshore Road, Ste-Anne-de-Bellevue, Quebec, Canada H9X 3V9
[b] Forest, Range and Watershed Management Organization, Lashgark Road, Tehran, Iran

Received 5 April 2007; received in revised form 15 January 2008; accepted 16 January 2008
Available online 2 February 2008

Abstract

The Iranian Soil and Water Research Institute has been involved in mapping the soils of Iran and classifying landforms for the last 60 years. However, the accuracy of traditional landform maps is very low (about 55%). To date, aerial photographs and topographic maps have been used for landform classification studies. The principal objective of this research is to propose a quantitative approach for landform classification based on a 10-m resolution digital elevation model (DEM) and some use of an Advanced Spaceborne Thermal Emission and Reflection Radiometer (ASTER) image. In order to extract and identify the various landforms, slope, elevation range, and stream network pattern were used as basic identifying parameters. These are extractable from a DEM. Further, ASTER images were required to identify the general outline shape of a landform type and the presence or absence of gravel. This study encompassed a relatively large watershed of 451 183 ha with a total elevation difference of 2445 m and a variety of landforms from flat River Alluvial Plains to steep mountains. Classification accuracy ranged from 91.8 to 99.6% with an average of 96.7% based upon extensive ground-truthing. Since similar digital and ASTER image information is available for Iran, an accurate landform map can now be produced for the whole country. The main advantages of this approach are accuracy, lower demands on time and funds for field work and ready availability of required data for many regions of the world.

Keywords: Landform identification; Digital elevation model (DEM); Elevation range; Stream network; Golestan Dam watershed; Geographic information systems (GIS)

1. Introduction

Soil erosion by water is a complex mechanism which depends on various topographic, soil, climatic, hydrologic, land-use and land-cover properties (Cochrane and Flanagan, 2001). Physiographic attributes and soil properties have a direct influence on erosion caused by water. The study of landforms plays an important supportive role in ranking erosion potentiality and in developing soil and land-use maps (Van Remortel et al., 2004).

In Iran, soil survey and land evaluation studies were initiated in 1953 in conformity with an agreement between the Food and Agriculture Organization of the United Nations (FAO) and the Government of Iran (Dewan, 1967; Mahler, 1970). The Iranian Soil and Water Research Institute has been involved in mapping the soils of Iran and classifying landforms for the last 60 years. To date, aerial photographs and topographic maps have been used for such landform classification studies (Banaei, 1993). The resulting maps display nine major landforms as defined by an FAO report, (Dessaunettes et al., 1971; see Table 1).

In an initial field investigation following the procedures of Cochran (1985), 726 representative points within the Golestan dam watershed (Fig. 1) were chosen and checked for agreement with the above mentioned published maps. Results showed that correlation of proper landform identification between map and field location was only 55%. With the advent of more powerful computers and the greater availability of remotely sensed data at a smaller scale, the creation of landform maps can now be taken to a higher level. This paper presents the results of a digital approach to landform classification which has in-turn been checked for accuracy with extensive ground-truthing.

A digital elevation model (DEM) offers a common method for extracting vital topographic information needed to model soil erosion and water flow across a landscape (Zhu et al., 1997;

* Corresponding author. Fax: +1 514 398 8387.
E-mail address: Robert.Bonnell@mcgill.ca (R. Bonnell).

0169-555X/$ - see front matter © 2008 Elsevier B.V. All rights reserved.
doi:10.1016/j.geomorph.2008.01.011

Table 1
Landform classification scheme according to Dessaunettes et al. (1971)

Landform	Slope class	Elevation range	Specific characteristics	Land use
River Alluvial Plains (RP)	Less than 1%	See Fig. 5a	a) These landforms are close to a river. b) General slope direction is parallel to that of the river. The general shape of this landform is an elongated eclipse with the major axis parallel to the slope of the river. c) Usually these landforms are next to a meandering river.	Usually used for irrigated farming
Piedmont Plains (PD)	0–5%	See Fig. 5b	a) Since RP is really a subset of PD, then RP must be isolated first. b) The shape of PD is normally one of a strip with the long dimension parallel to the mountain range front. The transverse elevation cross-section of PDs is normally quite flat. c) PDs are restricted to areas with non- or slightly gravelly soils.	Usually used for irrigated or dryland farming
Gravelly Talus Fans (GFc)	0–5%	See Fig. 5b	a) GFc and GFr are as a result of a major water course or a number of smaller water courses running down to the foot of mountain range fronts.	Rarely used for irrigated or dryland farming
Gravelly River Fans (GFr)	Mostly 0–2%, occasionally 2–5% in the higher parts	See Fig. 5b	b) The shape of an individual GFc and GFr is usually triangular-shell shape. A group of GFc/GFr is normally one of a strip with the long dimension parallel to the mountain range front. The transverse elevation cross-section of these fans is clearly convex. c) GFc and GFr always have highly gravelly soils.	
Plateaux and Upper Terraces (TR)	0–12%, with local relief intensity feature slopes of up to 25%	See Fig. 5c		Tops usually used for dryland farming
Hills (H)	Mostly 8–25%	50–500 m		Usually grazing and/or forestry.
Mountains (M)	Over 25%	More than 100 m, mostly between 500 and 1500 m.		Usually grazing and/or forestry.
Lowlands[a] (LL)	Usually less than 1%	[a]	a) These landforms are located at the lowest elevations of watersheds. b) The transverse elevation cross-section of LL is nearly level and often concave. c) Usually the water-table level is above the ground surface. The ground and surface water tend to accumulate with subsequent accumulation of fine sediment and salts.	
Flood Plains[a] (FP)	Usually less than 1%	[a]	a) Usually these landforms are next to a river known to flood frequently. b) The transverse elevation cross-section of FP is nearly level. c) FPs are affected by incoming surface water flow.	

[a] Not found within the study area.

Pennock and Corre, 2001). Shary et al. (2002) defined 12 types of slope curvature that potentially can be used for landform classification. Ballantine et al. (2005) were able to differentiate six landform features (peak, ridge, pass, plane, channel and pit) from locally derived parameters (slope, cross-sectional elevations, and longitudinal, minimum and maximum curvatures). MacMillan et al. (2000) produced a landform classification system based on quantitative digital variables. They proposed a conceptual design for a multilevel, hierarchical system for automated landform classification (MacMillan et al., 2004). Yet, Dragut and Blaschke (2006) argued that, "the problem of scale of both spatial extent and resolution make single objective classifications of landscape at least problematic, maybe unfeasible".

Existing studies have used existing landform maps or aerial photographs to initiate training sites for supervised classification (Hengl and Rossiter, 2003; Ballantine et al., 2005; Bolongaro-Crevenna et al., 2005; Prima et al., 2006). All of the above studies have some limitations; size of study area is small (MacMillan et al. 2000), less accurate scale (Bolongaro-Crevenna et al., 2005; Prima et al., 2006), or use of aerial photos for training (Hengl and Rossiter, 2003).

The principal objective of this research is to propose a method for landform classification based on a 10-m resolution DEM and some use of an ASTER image. The study area is large (451 183 ha) with a total elevation difference of 2445 m and slope gradients ranging from flat to 60%. Further, no authors seem to have based their classification accuracy on ground-truthing to the degree presented in this paper.

2. Materials and methods

2.1. The study area

The Golestan dam watershed (Fig. 1) is one of the sub-basins of the Gorgan river watershed and is located in the northeast sector of the Golestan Province of Iran. It has an area of 4511.83 km^2 and is located between 55° 21′ and 56° 28′ E longitude, and 36° 44′ and 37° 49′ N latitude. The highest elevation above sea level is 2492 m and the lowest elevation is 47 m. In general the topography of the Golestan dam watershed is characterized by a complex combination of mountains, hills, plains and rivers. Different sedimentary rocks such as limestone, sandstone, shale, dolomite, and marl, along with conglomerate, loess sediments and alluvium cover the area.

Average annual precipitation ranges from 135 to 700 mm and potential evapotranspiration ranges from 1410 to 1787 mm

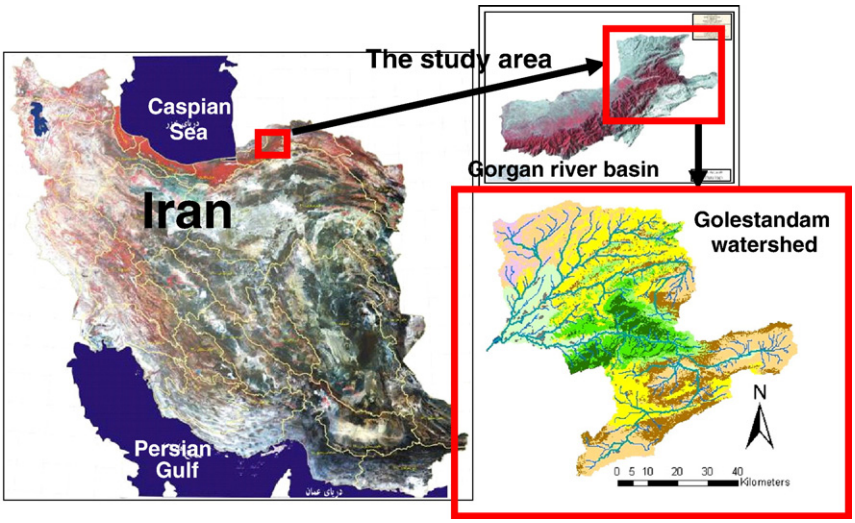

Fig. 1. Location of the study area.

(Japan International Cooperation Agency, 2005). Existing land-use and land-cover maps show rangeland with an area of 2014 km^2 (44.6% of whole study area), forest (973 km^2, 21.6%), dryland farming (1032 km^2, 22.9%), irrigated farming (461 km^2, 10.2%) and urban covering less than 1%. The main crops are wheat, barley, sunflower and watermelon.

Accelerated soil erosion, high sediment yield, floods and debris flow are serious problems in the Golestan dam watershed (Sharifi et al., 2002).

2.2. Preprocessing of existing data and DEM generation

Digital topographic maps at a scale of 1:25 000 with 10 m contour lines, prepared by the National Cartographic Center of Iran and the Forest, Range and Watershed Management Organization (based on 1993 aerial photos), were obtained. For use in ArcGIS, these layers were converted to 'shape file' format and various features such as contour lines, streams, roads, cities and villages were separated into unique layers (Fig. 2, operation 1). From the individual files a mosaic map was prepared. This required some corrections to the contour lines for producing a uniform map as follows: a) modifying elevation values per contour line, b) removal of self overlap trough contour lines, c) correction of intersections between different contour lines, and d) checking code consistency for each line (Fig. 2, operations 2 and 3).

The creation of a DEM was performed using the interpolating method specifically designed for the creation of hydrologically correct digital elevation models (DEMs). This algorithm is based upon the ANUDEM interpolation method developed by Hutchinson (1989) in which the input consists of the digitized "corrected contours", the point data from the topographic map and the digitized stream network. ANUDEM generated a 'Hydrologically correct DEM'. In this process it is important to be certain that the pixel size is not too large. Otherwise it may happen that two contour lines will be located in the same pixel. By quantification of the density of the contour lines on the

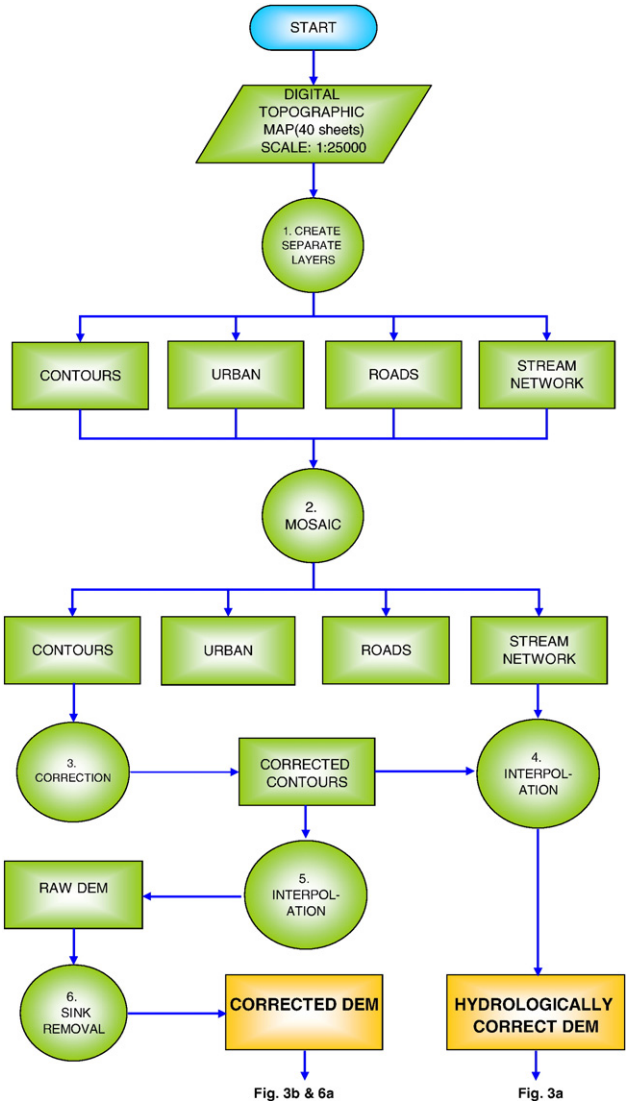

Fig. 2. Processing operations for DEM generation (flow diagram). For all flow diagrams: Circles = operation, Trapezoids = data input, Rectangles = maps or coverage and Diamonds = decisions.

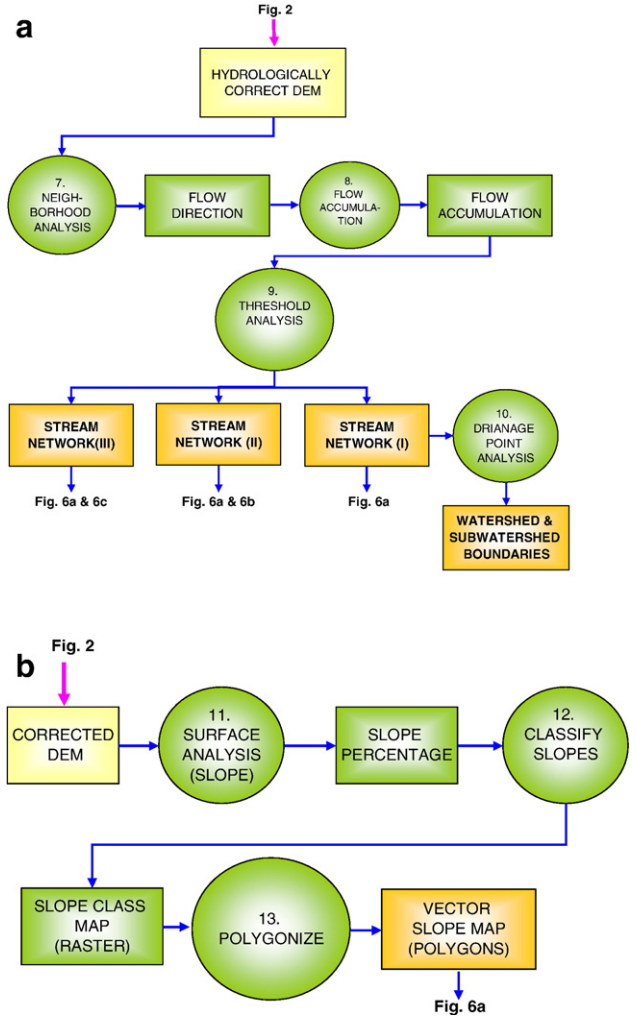

Fig. 3. Processing steps for (a) extracting stream network pattern and watershed boundaries, and (b) production of a slope map.

original hardcopy topographic map and trial and error, a square pixel size of 10 m was found to yield the best results. Since proper interpolation at the boundary of the study area requires knowledge of the contours just outside the actual study area, the DEM was extended 500 m outside the watershed. The resulting 'Hydrologically correct DEM' (Fig. 2, operation 4) was used in-turn to generate more detailed stream networks at three different scales (Section 2.3.1).

Use of the 'Hydrologically correct DEM' for generation of slope polygons resulted in many very small polygons adjacent to streams. At the scale of this study for landform classification, these very small polygons confused the situation. Thus it was decided to use a 'Raw DEM' without stream enforcement (Fig. 2, operation 5) but with 'sink removal' to generate a file termed the 'Corrected DEM' for use in generating slope polygons. A sink is a cell or set of spatially connected cells which has no surface outflow direction. This will occur when all neighboring cells are of a higher elevation, or when two cells flow into each other creating a two-cell loop. Sink removal (Fig. 2, operation 6) was performed following the fill method of Mark (1988).

2.3. Defining parameters required for the process of creating landform maps

Based upon the definitions of standard landform types in Iran, some essential parameters were used to identify and describe landforms (Table 1). These parameters, which include slope class, elevation range (ER = max. elevation − min. elevation within an area), and stream network pattern, play a vital role in landform classification. Slope class, elevation range and stream network pattern can be determined from a DEM. When these DEM-derived parameters were not sufficient for isolating unique landform polygons, the "specific characteristics" shown in Table 1 were utilized (details below). For this step, an ASTER image was used to visually identify the general outline shape of a landform polygon and the presence or absence of gravel.

2.3.1. Extracting stream network pattern, watershed points and watershed polygons

Stream network pattern and their drainage areas have an important supportive role in differentiating such landforms as River Alluvial Plains (RP), Gravelly Talus Fans (GFc), Gravelly River Fans (GFr), and River Terraces (TRr). For example River Alluvial Plains are formed by over-bank deposition of fine deposits by larger water course.

Hydrologically correct DEMs can be used to derive flow direction, flow accumulation, stream networks and watershed boundaries (Fig. 3a, operations 7, 8, 9 and 10). A neighborhood analysis was performed to generate a flow direction map. The results of flow accumulation were used to create three stream network levels by applying three threshold values (Tarboton et al., 1991; Garbrecht and Martz, 1994; Hogg et al., 1997). The main streams (stream network I) of the study area were extracted by using a threshold equal to 1% of the total cells (455 392 cells) in the whole watershed. The smallest streams (stream network III) were identified by using a threshold equal to 150 cells (150 cells represent 1.5 ha). According to Soil Survey Staff (1993), the smallest practical area of any identifiable feature on a 1:25 000 map represents 1.6 ha (0.5 by 0.5 cm). Between stream network I and the stream network III, stream network II was extracted by using a threshold equal to 45 000 cells (45 000 cells, or 450 ha).

This study encompassed a relatively large watershed of 451 183 ha which included a variety of landforms, geology,

Table 2
Land slope classes created from a DEM

Class no.	Slope range (%)
1	<1
2	1–<2
3	2–<5
4	5–<8
5	8–<12
6	12–<15
7	15–<25
8 [a]	25–<40
9 [a]	40–<60
10 [a]	≥60

[a] Classes 8, 9 and 10 are clumped (≥25%) for landform classification in this study, but are uniquely useful for erosion quantification in further studies.

soils, climatic conditions, hydrologic conditions, land-use and land-cover properties. In order to visit a full variety of landform types across the whole study area, the Golestan dam watershed was divided into seven sub-watersheds. The watershed and sub-watershed boundaries were extracted by using drainage points (junctions of streams) and watershed points (those junctions chosen as outlets of the seven sub-watersheds). The Madarso and Tamar rivers join just above Golestan dam lake; this was taken as the outlet for the full watershed. Thus the full watershed was divided into seven major sub-watersheds; three correspond with existing hydrologic stations.

2.3.2. Extracting the slope map

Slope steepness is a fundamental parameter in many soil erosion models (Warren et al., 2004). The processing steps for production of a slope map are shown in Fig. 3b. Slope gradient was calculated for each grid cell to the nearest degree of arc by the slope command in the ArcInfo (version 9) operating on a 3×3 matrix of neighboring elevations based upon an improved method of Horn (1981) (Fig. 3b, operation 11). Based upon the parameter requirement for landform classification as shown in Table 1, the land slopes were classified into eight categories (Fig. 3b, operations 12 and 13). For future soil erosion quantification studies, the last class (>25%) of land slope was subdivided into 25–39%, 40–59% and ≥60%. The results are shown in Table 2. The resulting corrected DEM, hill-shade, stream network and slope map are shown in Fig. 4.

2.3.3. Determining elevation range

As indicated in Table 1, local elevation range is another parameter used to identify landform types. Elevation range alone was found to be sufficient to identify hill and mountain areas.

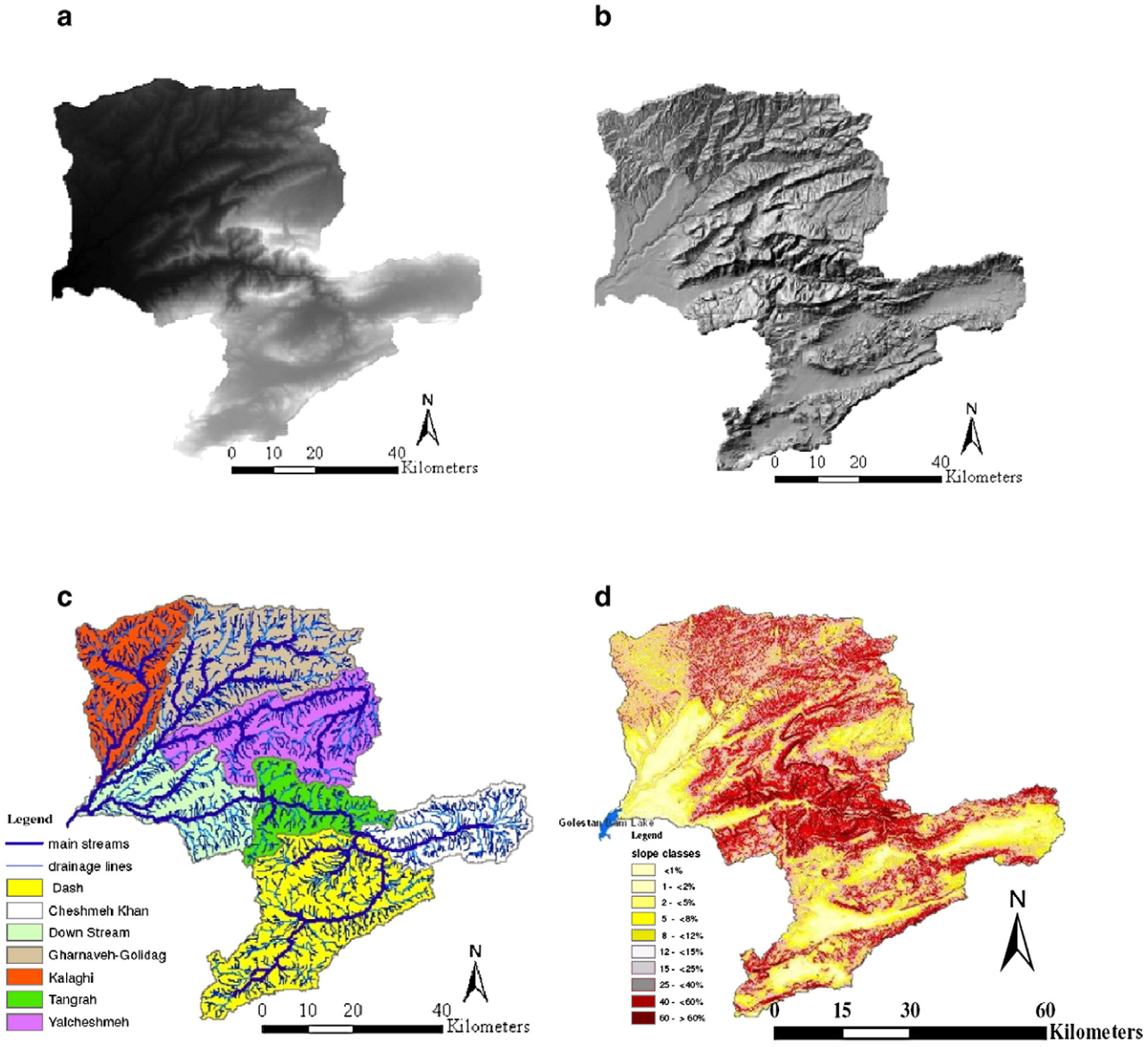

Fig. 4. Data required in the process of creating a landform map: (a) raster image of the corrected DEM with a square cell size of 10-m, (b) hill-shade (c) stream networks and sub-watersheds, and (d) vector slope map.

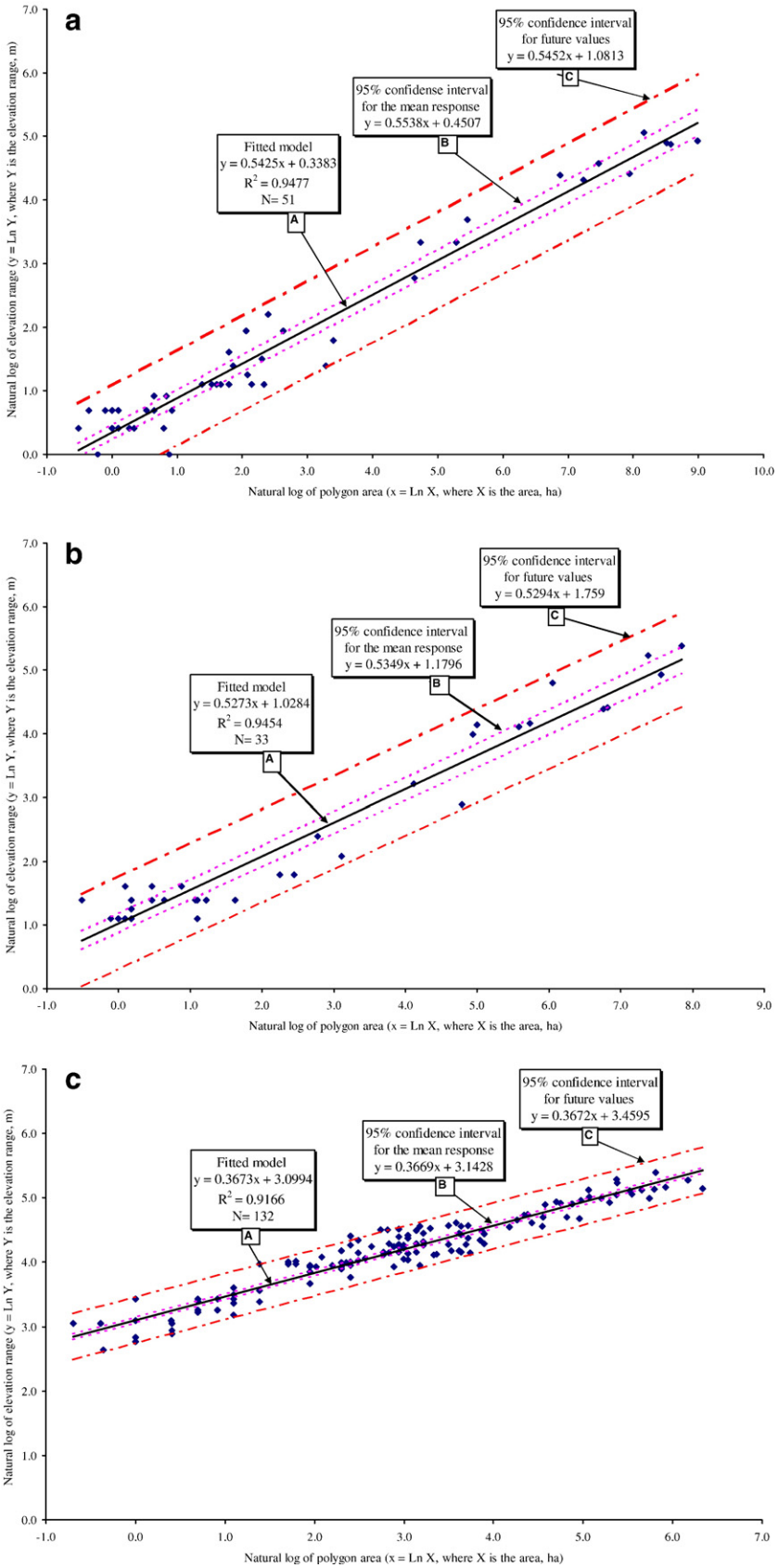

Fig. 5. Relationship between area and elevation range within (a) River Alluvial Plains, (b) Piedmont Plains and Gravelly Fans, and (c) Plateaux and Upper Terraces.

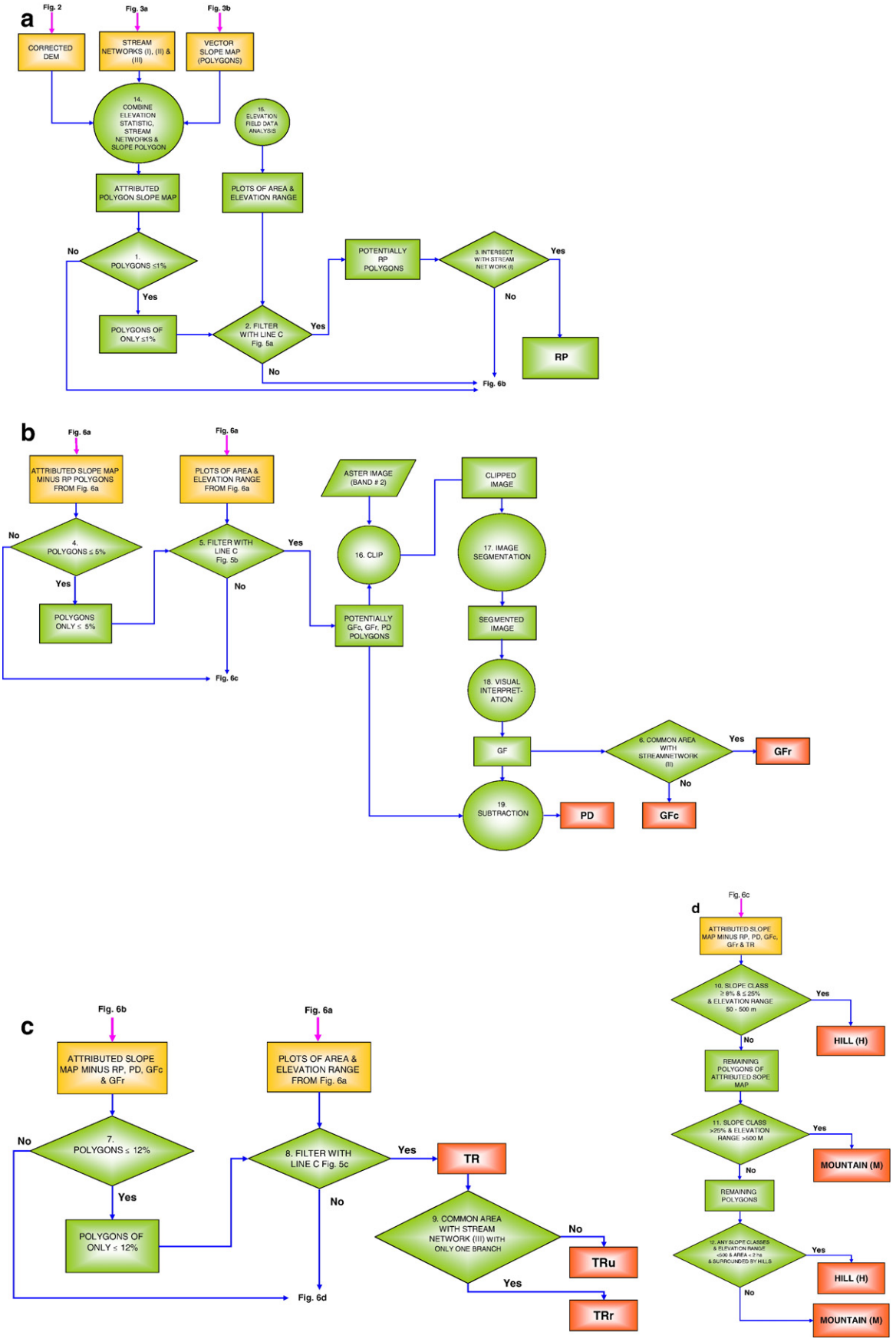

Fig. 6. Processing steps for extracting (a) River Alluvial Plains, (b) Piedmont Plains, Gravelly Talus Fans and Gravelly River Fans, (c) Plateaux and Upper Terraces, and (d) Hills and Mountains.

Table 3
Predicted elevation ranges (ER) based upon best fit lines of Fig. 5 (line A)

Polygon area (A) (ha)	Elevation range (m)		
	River Alluvial Plains (RP)	Plateaux and Upper Terraces (TR)	Piedmont Plains and Gravelly Fans (PD, GF)
$A \leq 2$	ER < 2.1	ER < 28.6	ER < 4.1
$2 < A \leq 5$	ER < 3.4	ER < 40.1	ER < 6.5
$5 < A \leq 10$	ER < 4.9	ER < 51.7	ER < 9.4
$10 < A \leq 50$	ER < 11.7	ER < 93.3	ER < 22.1
$50 < A \leq 100$	ER < 17.1	ER < 120.4	ER < 31.7
$100 < A \leq 200$	ER < 24.9	ER < 155.3	ER < 45.7
$200 < A \leq 500$	ER < 40.9	ER < 217.5	ER < 74.1
$500 < A \leq 1000$	ER < 59.5	ER < 280.5	ER < 106.8
$1000 < A \leq 2000$	ER < 86.7	ER < 361.8	ER < 153.9
$2000 < A \leq 5000$	ER < 142.5	ER < 506.6	ER < 249.5

Another approach was required for the other five landforms found in the study area. To address this, extensive field topographic data was collected. Using the slope polygon map, various polygons in the field were visited and at each location identified the polygon as RP, TR, PD or GF. Fifty-one typical RP, 132 typical TR and 33 typical PD and GF in the study area were so identified in the field. Then using a GPS unit elevation above sea level, longitude and latitude were measured at locations chosen to be near but inside the edge of each slope polygon (5 to 15 such locations, depending on the size of the polygon). Then, using this field data, geostatistics was used to determine elevation range and area of these field-identified polygons.

Plots of this data plus regression analysis lines and confidence intervals are shown in Fig. 5. It can be seen that there is a different relationship between polygon area and elevation range for each of RP, TR, PD and GF. The confidence intervals were established using the approach of MacBerthouex and Brown (2002) for joint confidence regions. The first interval (B), based upon the mean response is more restrictive since it is based solely upon the population mean error. The larger second interval (C) includes the mean response error plus measurement error. Using zonal statistics, minimum, maximum, range and mean elevation above sea level were extracted from the slope map for each polygon (Fig. 6a, operation 14). As an example, predicted elevation ranges based upon best fit line (Fig. 5, line A) and 95% confidence interval for future values (Fig. 5, line C) for various polygon sizes of RP, TR, PD and GF were computed (Tables 3 and 4). As discussed below these relationships were subsequently used to help identify landform types.

2.4. Extracting and identifying landform types

To start this process one must first note that in Table 1 River Alluvial Plains (RP) has a slope class of 0–1% and Plateaux and Upper Terraces (TR) have a slope class of 0–12%. Because of this overlap in slope classes, slope alone cannot differentiate the flatter landform types. Use must be made of more parameters. To isolate unique landform polygons, the approach used was to start with the flatter landform types. The best order of analysis was found to be slope, elevation range, stream network pattern, neighbourhood analysis and if needed visual interpretation of satellite images (in a future paper the authors plan to present an algorithm for this last step).

2.4.1. River Alluvial Plains (RP)

River Alluvial Plains are formed by over-bank deposition of fine deposits by a major water course. Here, 'major' refers to stream areas of 4500 ha or more. For this study region, stream areas less than 4500 ha always had slopes greater than 1%, thus excluding them from class RP. First, all polygons satisfying the slope requirement of less than 1% were extracted (Fig. 6a, decision #1). Then those plotting below the line C (Fig. 5a) for 95% confidence interval were isolated and classed as potentially RP (Fig. 6a, decision #2). Then, of these polygons, those intersected by a major water course were definitively classed as RP (Fig. 6a, decision #3). The rest fell under consideration for PD, GF and TR.

2.4.2. Piedmont Plains (PD) and Gravelly Talus Fans (GFc) and Gravelly River Fans (GFr)

The processing steps for extracting PD, GFc and GFr are shown in Fig. 6b.

The PD, GFc and GFr polygons are those with 0–5% slope (Fig. 6b, decision #4) and elevation ranges below line C of Fig. 5b (Fig. 6b, decision #5). The GFc and GFr subsets were isolated by use of ASTER images using Band #2 (Leica Geosystem, 2003). The final choice of Band #2 was taken because this band gave the best image for visual differentiation between PD, GFc and GFr. The ASTER image was first clipped to match the coverage of the potentially PD, GFc and GFr map (Fig. 6b, operation 16). Operation 17 consisted of taking the clipped image and via ERDAS "image segmentation" polygons of like reflectance were created. In this study image segmentation was performed by using Bonnie Ruefenacht algorithm (Ruefenacht, 2002). Operations 18 and 19 consisted of taking the segmented polygons and visually (using colour and shape) to separate GFc and GFr from PD (noting that GFc and GFr are normally distinctly triangular-shell in shape). GFc and GFr were themselves differentiated by use of associated stream network

Table 4
Predicted elevation ranges (ER) based upon 95% confidence interval for future values (Fig. 5, line C) for various polygon sizes of RP, TR, PD and GF

Polygon area (A) (ha)	Elevation range (m)		
	River Alluvial Plains (RP)	Plateaux and Upper Terraces (TR)	Piedmont Plains and Gravelly Fans (PD, GF)
$A \leq 2$	ER < 4.3	ER < 41.0	ER < 8.4
$2 < A \leq 5$	ER < 7.1	ER < 57.4	ER < 13.6
$5 < A \leq 10$	ER < 10.3	ER < 74.1	ER < 19.6
$10 < A \leq 50$	ER < 24.9	ER < 133.7	ER < 46.1
$50 < A \leq 100$	ER < 36.3	ER < 172.5	ER < 66.5
$100 < A \leq 200$	ER < 52.9	ER < 222.5	ER < 95.9
$200 < A \leq 500$	ER < 87.3	ER < 311.5	ER < 155.8
$500 < A \leq 1000$	ER < 127.4	ER < 401.8	ER < 224.9
$1000 < A \leq 2000$	ER < 185.9	ER < 518.3	ER < 324.7
$2000 < A \leq 5000$	ER < 306.4	ER < 725.6	ER < 527.4

size (decision #6). Those polygons found to be intersected by small stream networks (networks of less than 450 ha) were classed as GFc and those with larger networks (larger than 450 ha) were classed as GFr. This arbitrarily established classification limit (450 ha) was found to be effective for this study area, and may need calibration/adjustment for significantly different geomorphologic regions.

2.4.3. Plateaux and Upper Terraces (TR)

Once RP, PD, GFc and GFr were identified, the remaining area with less than 12% slope (Fig. 6c, decision #7) and plotting below line C in Fig. 5c (decision #8 in Fig. 6c) were classified as potentially "Plateaux and Upper Terraces" (TR). A further subdivision into Upper Terraces (TRu) and River Terraces (TRr) was possible. TRr were found to be those polygons intersected by a drainage line and having an area of less than 5 ha. All other polygons were then classified as TRu (Fig. 6c, decision #9). This finer classification was found to be useful in a related study in that TRu land-use and erosion potential were found to be different than those of TRr.

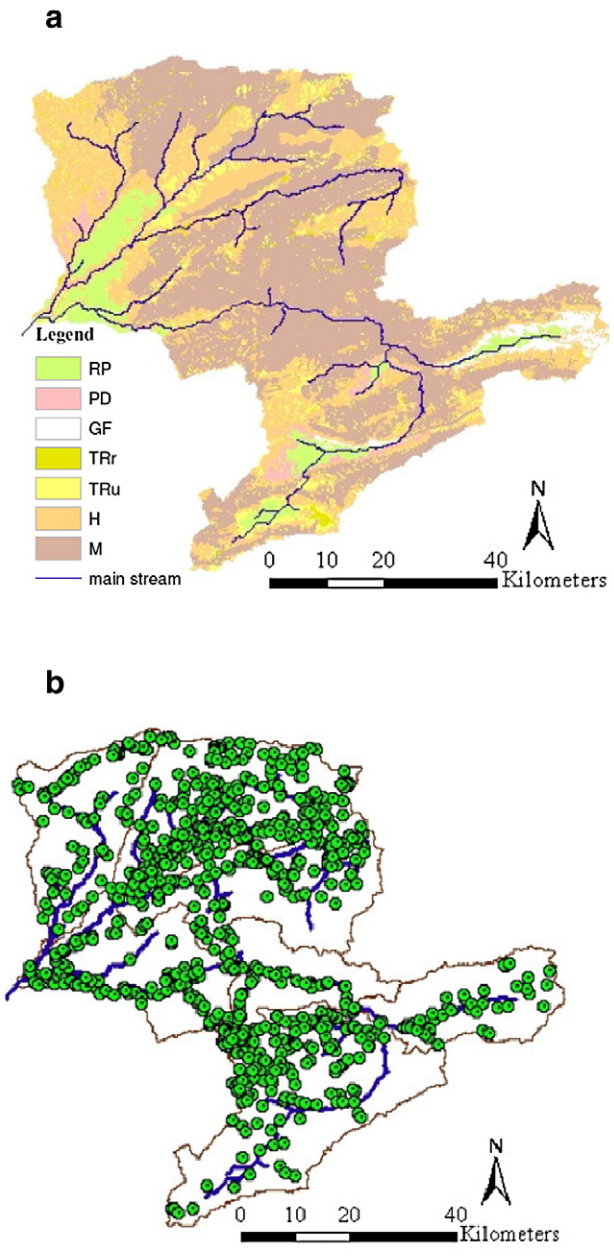

Fig. 7. Landform map and evaluation. (a) Landform map, (b) locations of the ground-truthing points used.

Table 5
Decision process for selecting 726 of 5805 polygons to visit in ground-truthing

	Area (ha)	Number of polygons in size range	% of total area	Cumulative area %	Polygon[a] visits	Number of sites to visit
1	$42\,000 \geq A > 20\,000$	5	37.7	37.7	10	50
2	$20\,000 \geq A > 10\,000$	9	27.8	65.5	6	54
3	$10\,000 \geq A > 5000$	5	7.2	72.7	5	25
4	$5000 \geq A > 1000$	18	12.4	85.1	4	72
5	$1000 \geq A > 500$	14	2.4	87.5	2	28
6	**$500 \geq A > 77$**	**107**	**4.3**	**91.8**	**1**	**107**
7	$77 \geq A > 40$	110	1.4	93.2	50%	55
8	$40 \geq A > 20$	264	1.6	94.8	35%	93
9	$20 \geq A > 10$	548	1.7	96.5	20%	110
10	$10 \geq A > 5$	1031	1.6	98.1	7%	73
11	$5 \geq A > 2$	2206	1.5	99.6	2%	44
12	≤ 2	1488	0.4	100	1%	15
Total	451 183	5805	100	100	12.5%	726

Line 6 is rendered in bold because this is the average area size.
[a] Number of visits per polygon if over mean size (77 ha) or % of polygons to visit if under mean size.

2.4.4. Hills (H)

The Hill polygons are those with 8–25% slope and 50–500 m elevation range (Fig. 6d, decision #10). Usually a number of polygons with steep slopes (>25%) and/or low elevation range (less than 50 m) were located at least partially within Hill polygons. In this case, if they were small polygons, they were classified as Hill (Fig. 6d, decision #12). Small, in this case, refers to all polygons less than 2 ha in size. Again this site-specific parameter may need to be changed for significantly different geomorphologic regions.

2.4.5. Mountains (M)

The Mountain polygons are those with slopes greater than 25% and high elevation range (Fig. 6d, decision #11). The difference of elevation between higher parts (ridge tops) and lower parts (valley bottoms) is more than 100 m, mostly between 500 and 1500 m. Usually a number of polygons with lower slopes (8–25%) were located at least partially within Mountain polygons. In this case, they were classified as Mountain (Fig. 6d, decision #12).

3. Evaluating accuracy of the landform map

Upon completion of all steps in Section 2.4, a landform map was created (Fig. 7a). For ground-truthing, polygons to visit were chosen to encompass a full variety of landform types across all seven sub-watersheds. A simple random sampling

Table 6
Determining distribution of polygon sites to visit across landform types and across sub-watersheds

Landform type	RP		PD		GF		TRr		TRu		H		M		Total	
Sub-watershed	T[a]	V[a]	T	V	T	V	T	V	T	V	T	V	T	V	T	V
Cheshme-Khan	–	–	–	–	–	–	1	–	6	2	20	7	–	–	27	9
Dasht	–	–	–	–	–	–	2	1	40	14	11	4	2	1	55	20
Down-stream	1	1	–	–	–	–	2	1	31	11	14	5	1	1	49	18
Garnaveh	1	–	2	1	–	–	5	2	37	13	4	1	–	–	49	17
Kalagi	–	–	–	–	–	–	12	4	14	5	2	1	1	–	29	11
Tangrah	–	–	–	–	–	–	1	–	2	1	6	2	–	–	9	3
Yalcheshme	–	–	1	–	–	–	14	5	30	10	1	–	–	–	46	15
Total	2	1	3	1	–	–	37	13	160	56	58	20	4	2	264	93

This table is an example for line 8 of Table 5.
[a] T = Total polygons, V = number of polygons to visit.

location approach would lead to two major problems. The first being some locations would take days to get to since there are no roads nearby. The second is that a simple random approach would give too much weight to small polygons; 63% of the 5805 polygons represent only 2% of the whole study area. Thus the following approach was used: all polygons larger than the overall mean polygon size of 77 ha were visited at one or more locations (Table 5). Below the mean size (77 ha), a certain percentage (from 50% for larger to 1% for the smallest) was chosen to be visited.

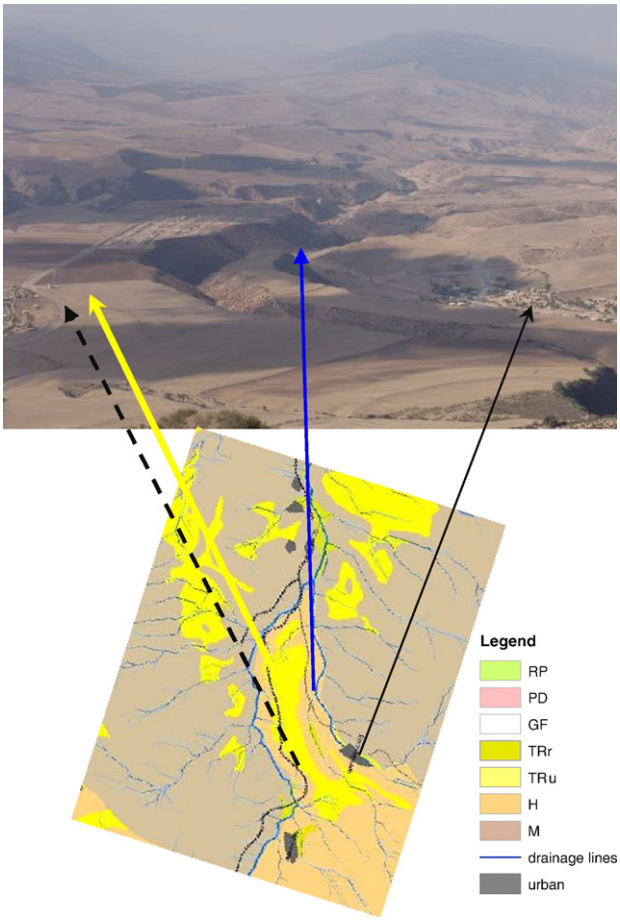

Fig. 8. Comparison between the landform map and a photograph of the same area.

Table 7
Error matrix of DEM-derived landform map and ground-truthing points

Landforms	Ground-truthing points							New classified
	RP	PD	GF	TRr	TRu	H	M	
River Alluvial Plains (RP)	56	0	0	0	0	0	0	56
Piedmont Plains (PD)	2	27	0	0	0	0	0	29
Gravelly Fans (GF)	0	0	28	0	0	0	0	28
River Terraces (TRr)	0	1	0	59	0	0	0	60
Upper Terraces (Tru)	0	0	0	0	122	0	1	123
Hills (H)	3	1	1	0	2	175	0	182
Mountains (M)	0	0	0	1	0	2	245	248
Total sites visited	61	29	29	60	124	177	246	726

The spread of polygon visits over all landform types and sub-watersheds is detailed in Tables 5 and 6. As an example, line 8 of Table 5 shows a plan to visit 93 or 35% of the total 264 polygons of this size range. Of the 264 total, 58 are Hills, so 20 (35%) should be visited (Table 6). This same percentage was used to distribute visits across sub-watersheds (Table 6). For example, 35% or four of the 11 polygons within the Dasht sub-watershed were to be visited. These four were randomly selected from the total 11, after having eliminated those polygons which for physical barriers or time constraints were essentially inaccessible.

Ground-truthing was attended by the first author and a field technician with 32 years of landform classification experience. In total, 726 points were visited (Fig. 7b) and using the attributes listed in Table 1 (slope, elevation range and specific characteristics) the landform at each point was classified.

4. Results and discussion

The landform map created using the steps of Section 2.4 is shown in Fig. 7a. Further a mountain-top photograph is matched with the corresponding section of the landform map (Fig. 8). In a qualitative sense good agreement is evident; the yellow Upper Terraces (TRu) are separated from drainage lines by narrow polygons of Hills. Even the DEM streamlines agree very well with those in the photograph. The map in Fig. 7a shows 5805 polygons; River Alluvial Plains with a total area of 30 743.6 ha (6.8% of the whole study area), Piedmont Plains (8038.7 ha, 1.8%), Gravelly

Table 8
Accuracy totals of DEM-derived landform map and ground-truthing points

Landform	Total sites visited (V)	Number correctly identified (C)	New classified (N)	Producer's accuracy (P_p)% $P_p = C_i/V_i$	User's accuracy (P_u)% $P_u = C_i/N_i$
River Alluvial Plains (RP)	61	56	56	91.8	100.0
Piedmont Plains (PD)	29	27	29	93.1	93.1
Gravelly Fans (GF)	29	28	28	96.6	100.0
River Terraces (TRr)	60	59	60	98.3	98.3
Upper Terraces (TRu)	124	122	123	98.4	99.2
Hills (H)	177	175	182	98.9	96.2
Mountains (M)	246	245	248	99.6	98.8
Total	726	712	726		

Overall classification accuracy = 98.1%.

Fans (8654 ha, 1.9%), Upper Terraces (33 664.2 ha, 7.5%), River Terraces (8230 ha, 1.8%), Hills (139 630 ha, 30.9%) and Mountains covering 222 222.5 ha, 49.3%.

It was found that, of the 726 points visited in the field, 98.1% correlated correctly with the map classification (Tables 7 and 8). The 'producer's accuracy' (Table 8) is a measure of how well the DEM process correctly identified a specific landform type; this ranged from a low of 91.8% to a high of 99.6% with an average of 96.7%. The 'user's accuracy' is a measure of how well the DEM process captured all occurrences of any specific landform type; this ranged from a low of 93.1% to a high of 100% with an average of 97.9%. These two 'accuracy' parameters were derived using the procedure of Congalton (1991).

The lowest and the highest producer's accuracy are for River Alluvial Plains (RP) and Mountains (M), respectively (Table 8). River Alluvial Plains (RP), along with Piedmont Plains (PD) and Gravelly Fans (GF), all have low slope values which greatly overlap and have similar elevation ranges. Thus they are somewhat easier to misclassify. Mapping these landforms is therefore much more dependent on how well the specific characteristics (Table 1) are defined and selected. Conversely, Mountains (M), Hills (H), and Plateaux and Upper Terraces (TR), which have the highest producer's accuracy, also have steeper slopes with much less slope overlap and larger elevation ranges. This tends to make them easier to classify correctly.

Piedmont Plains have the lowest user's accuracy, but this could be a result of the small population size. Hills also have a relatively low user's accuracy. This could be the result of the slope of Hills. Such long, narrow polygons can be misclassified as either RP, PD, or GF.

Most methods of automated landform classification have recognized individual landform elements based on morphometric parameters. Prima et al. (2006) defined five basic landform types (volcanoes, alluvial fans, alluvial plains, mountains and hills) using four morphometric parameters (slope, aspect, convexity and concavity). Ballantine et al. (2005) were able to differentiate six landform features (peak, ridge, pass, plane, channel and pit) from locally derived parameters (slope, cross-sectional elevations, and longitudinal, minimum and maximum curvatures). MacMillan et al. (2000) produced a complex landform classification system based on quantitative digital variables. This resulted in a model with fifteen landform elements. In our research, a quantitative method was applied to classify seven major landform types including 'River Alluvial Plains (RP), Piedmont Plains (PD), Gravelly Talus Fans (GFc), Gravelly River Fans (GFr), Plateaux and Upper Terraces (Upper Terraces (TRu) and River Terraces (TRr)), Hills (H) and Mountains (M)' based on slope, elevation range, stream network pattern and some use of an ASTER image. Slope was used to define the initial polygon boundaries. Then these polygon boundaries are further defined by using elevation range and stream network information. These two parameters can cause some 'slope defined polygons' to be merged. Further in the case of PD and GF these two parameters along with visual interpretation of the ASTER images can cause a 'slope define polygon' to be dissected.

Pike (1988) and Iwahashi and Pike (2007) recognized that local elevation difference was a key criteria in distinguishing those landform types which have low local elevation range such as 'alluvial fans, flood plains, and river terraces'. In our study, based upon polygon size and elevation range data, different regression lines were generated for each landform type (RP, PD, GFc, GFr and TR).

$$y_{RP} \leq 0.5452 x_{RP} + 1.0813 \quad (1)$$

$$y_{PD/GF} \leq 0.5294 x_{PD/GF} + 1.759 \quad (2)$$

$$y_{TR} \leq 0.3672 x_{TR} + 3.4595 \quad (3)$$

where $y = \mathrm{Ln}\ Y$, Y is the elevation range (m), $x = \mathrm{Ln}\ X$, X is the polygon size (ha).

As discussed in Section 2.3.3, these relationships were subsequently used to identify landform types. These relationships between elevation range and various polygon sizes (up to 8000) were found to be effective for this study area. No slope defined polygon size in this study is larger than 8099 ha, only 5 are between 5000 and 8099, while 90% are less than 5 ha. The authors thus have no data on polygons over 8099 ha and have little data on polygons close to 8000 ha. To comment on the regression beyond 8000 ha is too speculate. More data is required on polygons over 8000 ha. Also it should be noted that the field topographic data was collected for the five landforms found in the study area only. Further work needs to be done, specifically for the elevation ranges for various areas of Lowlands (LL) and Flood Plains (FP).

As indicated in Table 1, RP has a slope class of 0–1%, PD and GF of 0–5%, and TR of 0–12%; these landform types have obviously overlapping slope classes. Thus it only makes sense to first separate RP (0–1%) knowing that the rest will belong to PD and GF (0–5%) and TR (0–12%). Then to separate PD and GF (0–5%) and so forth. The conclusion is that it is best to start with the flatter landform.

5. Conclusions and recommendations

This study encompassed a relatively large watershed of 451 183 ha which included a variety of landforms, from flat River Alluvial Plains to steep mountains (representative of conditions in Iran), all well distributed across the watershed. In order to extract and identify the various landforms, land characteristics of slope, elevation range and stream network pattern were used as basic identifying parameters. These are available for extraction from a DEM. Further, ASTER images were required to identify the general outline shape of a landform type and the presence or absence of gravel (specifically for GFc and GFr).

Usually it is the low sloped landforms, such as River Alluvial Plains and Piedmont Plains that are the most difficult to differentiate via computer approaches. Yet this study found that landforms with overlapping and relatively flat slope characteristics could be separated into three distinct categories based upon polygon size and elevation range data.

The key conclusion to be drawn is that the authors have presented a quantitative approach for landform classification

based upon a DEM and some interpretation of an ASTER image. Classification accuracy ranged from 91.8 to 99.6%; based upon extensive ground-truthing.

In Iran and other countries, the study of landforms plays an important supportive role in developing soil, land-use and soil erosion maps. Traditional landform classification has been based on qualitative descriptions from surface shapes on aerial photographs. The approach presented here produces landform maps with an overall accuracy of 98.1%, far greater than the 55% accuracy ratio of the traditional methods. Since digital and ASTER image information is available for all of Iran, an accurate landform map can now be produced for the whole country. The main advantage of this approach is accuracy and lower demands on time and funds.

Acknowledgements

The authors gratefully acknowledge the Forest, Range and Watershed Management Organization of Iran and the Watershed Management Office of Golestan Province for providing available datasets and facilities, manpower and field support for this study. Many thanks to Mr. Adnan Azarshab for his intensive contributions to the field work and to Mr. Hossein Ali Mohammadi for his collaboration. We are grateful for the constructive comments given by Dr. Robert MacMillan, Dr. Richard J. Pike and an anonymous reviewer of our paper. We are also very thankful to Dr. Takashi Oguchi for his valuable comments and suggestions. Partial funding for this study came from the Natural Sciences and Engineering Research Council of Canadian.

References

Ballantine, J.A.C., Okin, G.S., Prentiss, D.E., Roberts, D.A., 2005. Mapping North African landforms using continental scale unmixing of MODIS imagery. Remote Sensing of Environment 97, 470–483.

Banaei, M.H., 1993. A report on soil survey, land classification and irrigation capability for a region located south of the Gorgan River. Publication No. 368. Soil and Water Research Institute of Iran, Tehran. (In Farsi).

Bolongaro-Crevenna, A., Torres-Rodriguez, V., Sorani, V., Frame, D., Ortiz, M.A., 2005. Geomorphometric analysis for characterizing landform in Morelos State, Mexico. Geomorphology 67, 407–422.

Cochran, W.G., 1985. Sampling techniques, 3rd Ed. John Wiley and Sons, New York.

Cochrane, T.A., Flanagan, D.C., 2001. Deposition processes in a simulated rill. In: Ascough II, J.C., Flanagan, D.C. (Eds.), Soil Erosion Research for the 21st Century. Proceedings of the International Symposium. American Society of Agricultural Engineers, St. Joseph, MI, pp. 139–142.

Congalton, R.G., 1991. A review of assessing the accuracy of classifications of remotely sensed data. Remote Sensing of Environment 37, 35–46.

Dessaunettes, J.R., Ochtman, L.H.J., Van de Weg, R.F., 1971. Soil survey, classification and correlation guide for Iran. Food and Agriculture Organization of the United Nations, Rome, and Pilot Development Project of Soil Institute, Tehran, Iran. 177 pp.

Dewan, M.L., 1967. Interim report to the government of Iran on soil survey and land classification for irrigation development in Iran. Publication No. 100. Reprinted by Soil Institute of Iran, Tehran, Iran.

Dragut, L., Blaschke, T., 2006. Automated classification of landform elements using object-based image analysis. Geomorphology 81, 330–344.

Garbrecht, J., Martz, L.W., 1994. Grid size dependency of parameters extracted from digital elevation models. Computers and Geosciences 20, 85–87.

Hengl, T., Rossiter, D.G., 2003. Supervised landform classification to enhance and replace photo-interpretation in semi-detailed soil survey. Soil Science Society of America 67, 1810–1822.

Hogg, J., McCormack, J.E., Roberts, S.A., Gahegan, M.N., Hoyle, B.S., 1997. Automated derivation of stream-channel networks and selected catchment characteristics from digital elevation models. In: Mather, P.M. (Ed.), Geographical Information Handling: Research and Applications. Wiley, Chichester, pp. 211–235.

Horn, B.K.P., 1981. Hill shading and the reflectance map. Proceedings of the IEEE 69 (1), 14–47.

Hutchinson, M.F., 1989. A new procedure for gridding elevation and stream line data with automatic removal of spurious pits. Journal of Hydrology 106, 211–232.

Iwahashi, J., Pike, R.J., 2007. Automated classifications of topography from DEMs by an unsupervised nested-means algorithm and a three-part geometric signature. Geomorphology 86, 409–440.

Japan International Cooperation Agency, 2005. The study on flood and debris flow in the caspian coastal area focusing on the flood-hit region in Golestan Province. Interim Report. Tehran, Iran.

Leica Geosystem GIS and Mapping LLC, 2003. ERDAS Imagine (version 8.7) User Guides. Atlanta, USA.

MacBerthouex, P., Brown, L.C., 2002. Statistics for Environmental Engineers, 2nd Ed. CRC Press, Boca Raton, FL. 489 pp.

MacMillan, R.A., Pettapiece, W.W., Nolan, S.C., Goddard, T.W., 2000. A generic procedure for automatically segmenting landforms into landform elements using DEMs, heuristic rules and fuzzy logic. Fuzzy Sets and Systems 113, 81–109.

MacMillan, R.A., Keith Jones, R., McNabb, D.H., 2004. Defining a hierarchy of spatial entities for environmental analysis and modeling using digital elevation models (DEMs). Computers, Environment and Urban Systems 28, 175–200.

Mahler, P.J., 1970. Manual of land classification for irrigation. Publication No. 205. Soil Institute of Iran, Tehran, Iran.

Mark, D.M., 1988. Network models in geomorphology. In: Anderson, M.G. (Ed.), Modelling Geomorphological Systems. John Wiley & Sons, Chichester, pp. 73–97.

Pennock, D.J., Corre, M.D., 2001. Development and application of landform segmentation procedures. Soil and Tillage Research 58, 151–162.

Pike, R.J., 1988. The geometric signature: quantifying landslide-terrain types from digital elevation models. Mathematical Geology 20, 491–511.

Prima, O.D.A., Echigo, A., Yokoyama, R., Yoshida, T., 2006. Supervised landform classification of northeast Honshu from DEM-derived thematic maps. Geomorphology 78, 373–386.

Ruefenacht, B., 2002. Bonnie Ruefenacht algorithm. An Image Segmentation Algorithm Developed by the USDA Forest Service. Remote Sensing Application Center. http://www.fs.fed.us/.

Sharifi, F., Saghafian, B., Telvari, A., 2002. The great 2001 flood in Golestan province, Iran: causes and consequences. Proceedings of the International Conference on Flood Estimation. March 6–8, 2002. Berne, Switzerland, CHR-KHR Report 11-17, pp. 263–271.

Shary, P.A., Sharayab, L.S., Mitusov, A.V., 2002. Fundamental quantitative methods of land surface analysis. Geoderma 107, 1–43.

Soil Survey staff, 1993. Soil survey manual. Agricultural Handbook 18. United States, Department of Agriculture-Soil Conservation Service, Washington, DC.

Tarboton, D.G., Bras, R.L., Rodriguez-Iturbe, I., 1991. On the extraction of channel networks from digital elevation data. Hydrological Processes 5, 81–100.

Van Remortel, R.D., Maichle, R.W., Hickey, R.J., 2004. Computing the LS factor for the Revised Universal Soil Loss Equation through array-based slope processing of digital elevation data using a C++ executable. Computers and Geosciences 30, 1043–1053.

Warren, S.D., Hohmann, M.G., Auerswald, K., Mitasova, H., 2004. An evaluation of methods to determine slope using digital elevation data. Catena 58, 215–233.

Zhu, A.-Xing, Band, L., Dutton, B., 1997. Derivation of soil properties using a soil land inference model _SoLIM. Soil Science Society of America Journal 61, 523–533.